ELSEVIER

Carbohydrate Polymers 43 (2000) 215–222

Carbohydrate Polymers

www.elsevier.com/locate/carbpol

Rheological behavior of cross-linked waxy maize starch dispersions during and after heating

J. Tattiyakul, M.A. Rao*

Department of Food Science and Technology, Cornell University-Geneva, Geneva, NY 14456-0462, USA

Received 25 October 1999; received in revised form 14 January 2000; accepted 15 January 2000

Abstract

A model was developed to describe the complex viscosity versus temperature (η^*–T) data on 5% (w/w) cross-linked waxy maize (CWM) starch dispersions (STDs) obtained over the frequency range (ω) 1.26–31.38 rad s^{-1} and temperature range 55–95°C. The 5% CWM starch dispersions had an onset gelatinization temperature at 60°C with a peak complex viscosity (η^*_{peak}) of 6.9 Pa s at 64°C. The lowest post-gelatinization complex viscosity (η^*) was about $0.85\eta^*_{peak}$ at 80°C. The complex viscosity was related to the apparent viscosity using a Modified Cox–Merz rule. Flow tests on gelatinized 5% CWM STDs showed that the sample exhibited a combined time-dependent shear-thickening (antithixotropic) and time-dependent shear-thinning (thixotropic) behavior. The antithixotropic behavior, that appears to have resulted from a shear-induced structure formation, predominated when the level of shear stress imposed on the sample was less than 120–150 Pa.

Keywords: Starch dispersion; Viscosity; Shear stress; Time-dependent flow behavior

1. Introduction

Viscosity of starch dispersion is strongly influenced by swelling of starch granules. In turn, the swelling characteristic of starch granules primarily depends on the variety and source of the starch (Lineback, 1984; Swinkels, 1985). In high amylopectin cereal starches like waxy maize starch (ca. 99% amylopectin, Lineback, 1986), the granules tend to hydrate with ease, swell rapidly, and rupture to a great extent. As a result, the starch paste loses viscosity relatively easily producing weak bodied, stringy and cohesive pastes. Cross-linking treatment is intended to add chemical bonds at random locations within granules. These chemical bonds stabilize the granules and, hence, strengthen the relatively tender swollen starch granules. Cross-linked waxy maize starch pastes are more viscous and heavy bodied, and are less likely to breakdown with extended cooking times, increased acid or severe agitation (Langan, 1986).

Pasting history also affects consistency of the starch dispersion. Many studies showed that starch gelatinization is temperature and time dependent and can be explained by a pseudo-first-order Arrhenius kinetics (Kubota, Hosokawa, Suzuki & Hosaka, 1979; Lund & Wirakartakusumah, 1984; Okechukwu & Rao, 1995; Okechukwu, Rao, Ngoddy & Mcwatters, 1991). Winkler, Von S., Luckow and Donie (1971) employed a rotational viscometer to investigate the pasting properties of several starches. They observed a continuous change in paste viscosity throughout the non-isothermal pasting process and concluded that the pasting properties were sensitive to energy input and shear rate. According to Dolan and Steffe (1990), the major variables controlling the pasting process were temperature–time history before peak viscosity, strain history between peak viscosity and cooling, and temperature during cooling.

Starches have been classified into four types based on their gelatinized paste viscosity profiles (Schoch & Maywald, 1968). Type A is the group of high swelling starches (e.g. potato, tapioca, waxy cereal), which are characterized by a high viscosity peak followed by rapid thinning during cooking. Type B starches are moderate swelling starches, which show a lower pasting peak viscosity, and much less thinning during cooking (e.g. normal cereal starches). Type C starches are restricted swelling starches (e.g. chemically cross-bonded starches), which show a relatively less pronounced peak viscosity and exhibit high viscosity that remains constant or increases during cooking. Type D starches are highly restricted starches (e.g. high amylose corn starches), which do not swell sufficiently to give a viscous solution.

Yang and Rao (1998a) employed a dynamic rheological

* Corresponding author. Tel.: + 1-315-787-2266; fax: + 1-315-787-2284.

E-mail address: mar2@cornell.edu (M.A. Rao).

0144-8617/00/$ - see front matter
PII: S0144-8617(00)00160-0

test to measure the change in complex viscosity (η^*) throughout the course of starch gelatinization. η^* versus temperature (T) profiles of 3.5–8% corn STDs were obtained at various heating rates and oscillatory shear rates (ω). The results showed that increasing starch concentration (c) and decreasing ω resulted in a higher peak η^*. At a specific starch concentration, the η^*–T profiles exhibited the same shape and were reduced to a single master curve by using a shift factor concept of Ferry (1980). A comprehensive η^*–T model over a broad range of shear rates was proposed. The modified Cox–Merz rule (Eq. (1)) was later employed to relate η^* to apparent viscosity (η_a). As a result, a generalized η_a model involving the effect of temperature and shear rate ($\dot{\gamma}$) was obtained

$$\eta^*(\omega) = C[\eta_a(\dot{\gamma})]^{\alpha}\big|_{\omega=\dot{\gamma}} \quad (1)$$

This model was successfully employed in simulation of heat transfer and understanding broken heating phenomenon in a canned starch dispersion during sterilization (Yang & Rao, 1998b). The same modeling approach was used on waxy rice starch dispersion (Liao, 1998) and the model was also successfully applied in simulation of continuous sterilization of the starch dispersion.

Härröd (1989) reported both thixotropic and antithixotropic behaviors in 3–10% modified potato starch pastes and concluded that the behavior was strictly related to the magnitude of shear stress. Dintzis, Berhow, Bagley, Wu and Felker (1996) pointed out that shear-thickening properties were also sensitive to the solvent system, sample treatment, and starch composition. In samples that exhibited time-dependent shear-thickening, the behavior was more stable in the following order of solvents: 0.2N NaOH > 90% dimethyl sulfoxide (DMSO) with water > water or 0.5 N KCl at neutral pH. Also, samples that contained a large amount of amylopectin were able to form shear-induced networks that were responsible for shear thickening. Severe treatments, such as extended heating or vigorous stirring, of the sample generally destroyed the ability of the starch to form shear-thickened fluids. A shear-induced structure in the form of clusters in retorted 2.6% cross-linked waxy maize starch dispersion was visualized by light microscopic method (Chamberlain, Rao & Cohen, 1999). Scanning electron microscopy of raw cross-linked waxy maize starch; Purity W®, also revealed similar cluster formation (Holmes & Soeldner, 1981).

The main objectives of this study were: (1) to obtain a functional viscosity model of a CWM starch dispersion during gelatinization for use in thermal process calculation; and (2) to examine heated CWM starch dispersion's shear rate versus shear stress behavior with respect to thixotropic and antithixotropic behavior.

2. Materials

CWM (Purity W®, National Starch and Chemical Company (Bridgewater, NJ) starch dispersions (5, 6, 7, and 8% (w/w)) were prepared for use in the temperature sweep tests. All samples were allowed to sufficiently hydrate at room temperature for about 30 min before transferring to the rheometer plate.

To study applicability of the modified Cox–Merz rule and to examine the shear rate versus shear stress with respect to the time-dependent behavior of the STDs, gelatinized 5–8% STDs were prepared for frequency sweep tests and flow tests. Ungelatinized STDs in Erlenmeyer flasks were heated in a water bath to 70°C for 5 min with minimal agitation using a magnetic stirrer bar. The samples were allowed to reach room temperature before transferring to the rheometer plate.

3. Methods

Three types of rheological tests were performed: (1) to obtain η^* versus T profiles for the CWM starch dispersion, temperature sweep tests were carried out; (2) to establish a relationship between η^* and η_a of the STD, a frequency sweep followed by stepped-ramp shear flow tests were employed; and (3) to study flow behavior of the gelatinized STDs as affected by temperature and shear history, stepped shear flow tests were conducted. The rheological tests were done on a AR1000N® rheometer (TA Instruments, New Castle, DE). All measurements were done in triplicate.

3.1. Temperature sweep tests

These tests were conducted using the procedures described in detail earlier (Yang & Rao, 1998a). A parallel plate geometry (4 cm flat stainless steel plate with 500 μm gap) was used and the dispersion (0.64 ml) was transferred to the bottom plate by a micropipette. Water evaporation from the sample that occurs at high temperature was minimized by placing paraffin oil at the edge of the steel plate soon after gelatinization began. The sample was heated from 55 to 97°C at 2.1°C min^{-1} heating rate. The effect of oscillatory shear rate, ω, (1.26–31.38 rad s^{-1} for 5% STD) and concentration, c, (5, 6, 7, and 8% (w/w) at $\omega = 6.28$ rad s^{-1}) on rheological behavior of STD was investigated. The η^*, G', G'' and phase angle (δ) of the heated STD samples were measured as a function of temperature. Additional time sweep tests (5 min at 76°C and 5 min at 95°C) were done on a 5% sample to examine the influence of heating time.

3.2. Frequency sweep test versus flow test

For frequency sweep tests, a cone and plate geometry (6 cm diameter acrylic cone, 2°, 69 μm gap, sample amount = 2.16 ml) was employed. Prior to frequency sweep tests, a torque sweep experiment (at 20°C and 6.28 rad s^{-1}) was carried out to find the linear viscoelastic range (LVR) for the gelatinized STDs. The LVR of the heated 5% STD was found within 3% strain. Frequency sweep test was carried out in the LVR at 20°C and a

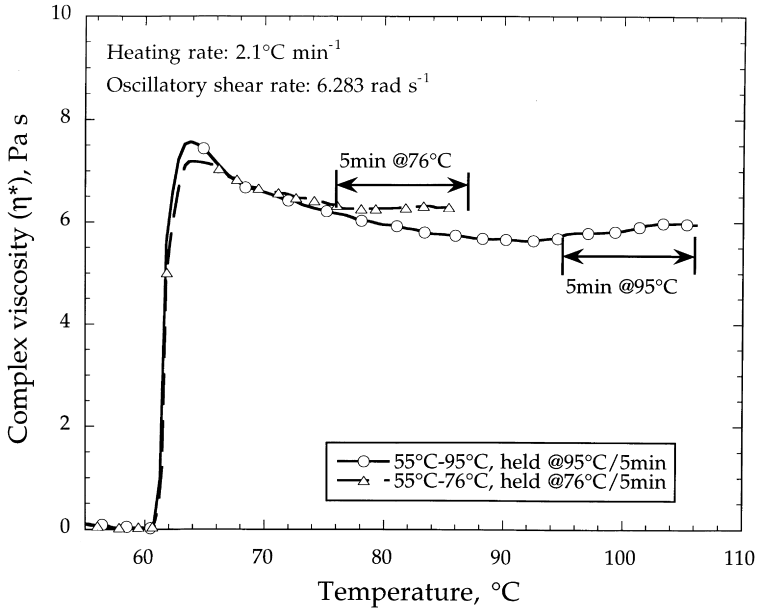

Fig. 1. Effect of holding time at 76 and 95°C on complex viscosity–temperature profiles of 5% cross-linked waxy maize starch dispersions: heating rate 2.1°C min^{-1}, 3% strain, and $\omega = 6.283$ rad s^{-1}.

frequency range of 0.63–125.7 rad s^{-1}. A stepped-ramp shear flow test was carried out over the same shear rate range (0.63–125.7 s^{-1}) and temperature (20°C) upon completion of the frequency sweep test.

3.3. Flow test

The flow behavior of gelatinized CWM STDs was determined using a cone and plate geometry. An acrylic cone (6 cm diameter 2°, 69 μm gap with solvent trap) was used in the flow tests at 20°C and a stainless steel cone (6 cm diameter steel cone, 2°, 78 μm gap with solvent trap) was employed in the flow tests at higher temperatures. After the sample was transferred to the rheometer plate, it was allowed to rest for 5 min before the flow test was started. Stepped-ramp shear rate in the range 0.1–500 s^{-1} was applied to the gelatinized STDs and the resulting shear stress was measured. Once the percentage of change in the shear stress was less than one for five consecutive times, a steady value of the resulting stress was reported. To determine the temperature effect on flow behavior of gelatinized CWM STD, gelatinized 5% STDs were tested at a shear rate range of 0.1–500 s^{-1} and 20–80°C. To determine the shear rate and shear history effects on flow behavior of the STD, gelatinized 5–8% CWM STDs were sheared at shear rate of 0.1–40 and 0.1–125 s^{-1}, respectively.

4. Results and discussion

4.1. Complex viscosity versus temperature profile

The η^* versus temperature profiles of 5% CWM STDs (Fig. 1) suggested CWM starch have characteristics similar to those of a type C starch (Schoch & Maywald, 1968). Gelatinized CWM STD showed a slight decrease in viscosity after the peak viscosity was reached.

Increasing temperature of the dispersion after the peak viscosity was attained resulted in a structural destruction of the gelatinized STD and, hence, a reduction of the STD viscosity (Yang & Rao, 1998a). Fig. 1 shows that the STD heated from 55 to 76°C and held at 76°C for 5 min had a higher final viscosity than the STD heated from 55 to 95°C and held at 95°C for 5 min. Therefore, the post-gelatinization viscosity of the STD was very sensitive to the heating temperature.

4.2. Effect of concentration on η^*–T profiles

An increase in the starch concentration resulted in a higher complex viscosity (figure not shown). A power relationship can be used to express the effect of concentration on the peak complex viscosity (η^*_{peak}). Similar relationship was successfully used to show the effect of concentration on apparent viscosity or consistency index of 4.7–7.1% pulp orange juice (Vitali & Rao, 1984), 5.8–30% tomato concentrates (Harper & El Sahrigi, 1965), and 3.5–8% cornstarch dispersions (Yang & Rao, 1998a). Morgan, Steffe and Ofoli (1989) proposed an exponential correlation between concentration (c) and apparent viscosity of protein dough during thermal processing which was successfully applied to starch solution in Dolan and Steffe's (1990) work. In this work, a power law relationship (Eq. (2)) was found to better represent starch the c–η^*_{peak} relationship

$$\eta^*_{peak} = 0.00585c^{4.34} \qquad R^2 = 0.994 \tag{2}$$

In addition, the integrated area under η^*–T curve over a

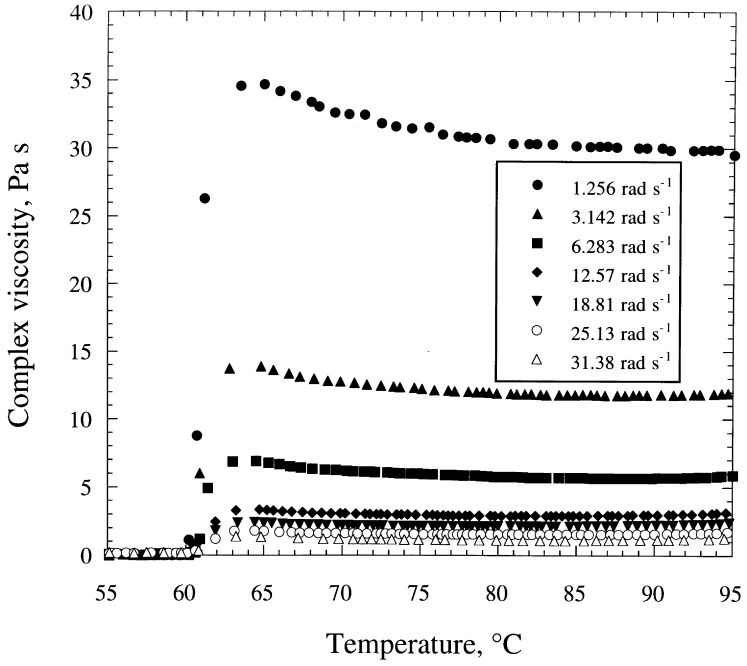

Fig. 2. Effect of frequency on complex viscosity–temperature profiles of cross-linked waxy maize starch dispersions heated from 55 to 97°C at 2.1°C min^{-1}. Data were obtained at 3% strain.

fixed temperature range can also be used to investigate the effect of concentrations on η^* (Liao, 1998). The areas under the complex viscosity versus temperature curves of the 5, 6, 7, and 8% CWM STDs in the temperature range 55–95°C were 203, 404, 897, and 1578 Pa s °C, respectively. A power correlation (Eq. (3)) was found between the area under the η^*–T profiles and starch concentration (c)

$$\text{Area under } \eta^*\text{–}T \text{ curve} = 0.121c^{4.56} \qquad R^2 = 0.998 \qquad (3)$$

Liao (1998) found a similar correlation with an exponent of 1.5 and a multiplying constant of 17.6 for 4, 6, and 8% waxy rice starch dispersions whose areas under η^*–T curves in the temperature range 55–95°C were 79.4, 262, and 406 Pa s °C, respectively. He suggested that magnitudes of the multiplying constants depend much more on the range of temperatures selected in the determination of the areas than those of the exponent.

4.3. Effect of oscillatory shear rate

The η^*–T profiles of 5% CWM STD obtained at values of ω from 1.26 to 31.38 rad s^{-1}, 3% strain, and a heating rate of 2.1°C min^{-1}, are shown in Fig. 2. As expected, an increase in ω resulted in a decrease in η^*. The η^*–T profiles at the different frequencies were similar in shape. Therefore, it was expected that a single master curve can be obtained by reducing the η^*–T profiles. By employing the scaling factor (Yang & Rao, 1998a); $(\omega/\omega_r)^{\beta}$, the reduced complex viscosity; η^*_R, was calculated:

$$\eta^*_R = \eta^*\left(\frac{\omega}{\omega_r}\right)^{\beta} \qquad (4)$$

where, ω is the oscillatory shear rate or frequency at which the test was performed, and ω_r is the reference oscillatory shear rate ($\omega_r = 6.283$ rad s^{-1}). The exponent of the shift factor, β, was determined by graphical shift of the experimental data obtained at different shear rates. Superposition of η^*_R and, hence, a master curve, was attained (Fig. 3) when η^*_R was plotted versus temperature at different ωs. The value of the scaling factor β was found to be 0.94 for the data at 18.81 and 25.13 rad s^{-1}, and 1.00 for the data at all other frequencies.

The following correlation was found to best describe the viscosity change over the course of gelatinization:

$$\eta^*\left(\frac{\omega}{\omega_R}\right)^{\beta} = \eta^*_{peak} \times \left(1 - \frac{1}{1 + \{m1 \times e^{m2\times(T-T_o)}\}}\right) \times \frac{1}{[1 + (T - T_p)^2]^{m3/T}} \qquad (5)$$

where, η^*_{peak} is the average peak complex viscosity at temperature T_p, which was equal to 6.9 Pa s at $T_p = 64$°C in this experiment, T_o is the gelatinization onset temperature; $T_o = 60$°C, and $m1$, $m2$, and $m3$ are constants equal to 0.0674, 2.332, and 2.1, respectively. A number of equations (Tattiyakul, 2000) were tested to describe the η^*–T data. However, Eq. (5) had the highest R^2 ($R^2 = 0.992$) and Chi square value of 2.57. Note that η^*_{peak} decreased only slightly after the peak temperature. The lowest average

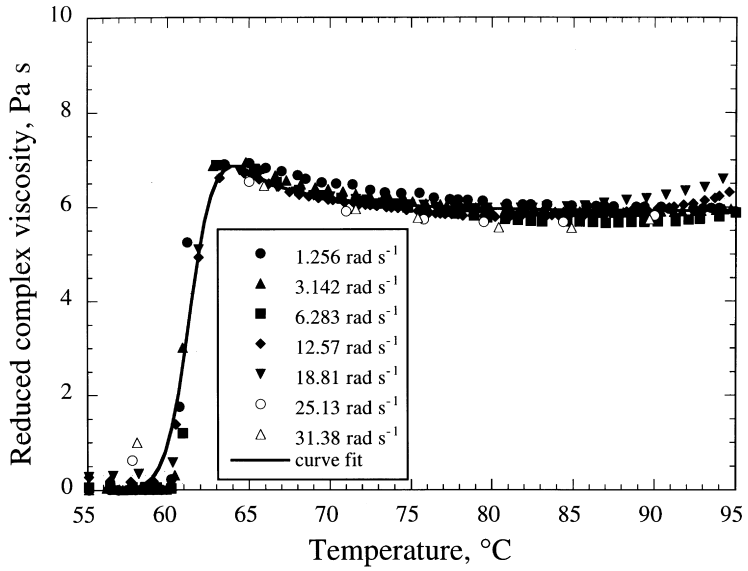

Fig. 3. Master curve of complex viscosity–temperature profiles of 5% cross-linked waxy maize starch dispersions heated from 55 to 95°C at 2.1°C min^{-1} heating rate, 3% strain, and $\omega = 1.256$ rad s^{-1}–31.38 rad s^{-1}.

post-gelatinization η^* observed from the master curve at ~80°C was 5.9 Pa s, which was about 85% of η^*_{peak}. After 80°C, η^* increased again and reached a value ~6.2 Pa s at 95°C. This was presumably due to time-dependent shear-thickening. Results of experiments that were performed to test the time-dependent behavior of the STD will be discussed later.

4.4. Cox–Merz rule: relationship between η^* and η_a

The Cox–Merz rule states that the η_a should be the same function of $\dot{\gamma}$ as η^* is of ω (Barnes, Hutton & Walters, 1989) and has been found to be useful where obtaining the experimental data from a dynamic rheological test is simpler than a steady shear experiment (Walters, 1975). To establish such a η^*–η_a relationship, the η^* and η_a data were obtained in the same shear rate range. Logarithmic plot of η^* and η_a versus shear rate showed two linear curves almost parallel to each other (figure not shown). Deviation from the Cox–Merz rule reflects the gel-like nature of gelatinized 5% CWM starch dispersions (Ross-Murphy, 1984). Rao, Okechukwu, Da Silva and Oliveira (1997) reported similar deviation from the Cox–Merz rule behavior in 3–5% modified waxy maize starch dispersions. The group observed that the dynamic viscosity (η') was in better agreement with the apparent viscosity than was η^*. In this case, the modified Cox–Merz parameters, C and α, were determined. The η^* and η_a data were better correlated using the modified Cox–Merz rule (Eq. (1)). For the 5% CWM STD heated to 70°C and held at 70°C for 5 min the constants C and α were found to be 1.796 and 1.346, respectively. Liao (1998) showed that the values of C and α did not vary significantly for starch gelatinized at different temperatures. By combining modified Cox–Merz rule and Eq. (5), a model for η_a of 5% CWM STD applicable to thermal processing was derived.

4.5. Time-dependent shear-thickening (antithixotropic) of gelatinized CWM starch dispersions

In addition to shear-thinning (pseudoplastic) behavior (Fig. 4), gelatinized 5% CWM STDs exhibited combined hysteresis loops, i.e. anticlockwise loop at low shear rates and clockwise loop at higher shear rates, when shear stress (σ) versus shear rate ($\dot{\gamma}$) data from both increasing-order (up) and decreasing-order (down) shear cycles (Fig. 5) were plotted. We note that an anticlockwise loop denotes antithixotropic and a clockwise loop denotes thixotropic behavior, respectively. The shear stress limits between the different kinds of time dependency appear to be specific for each starch type. Härröd (1989) reported that the limiting shear stress range of 10 ± 5 to 150 ± 50 Pa, in which antithixotropic behavior was switched on, was valid for samples from a broad range of preparation conditions. Outside this range, the samples showed thixotropic behavior.

Fig. 5 shows that gelatinized 5% CWM STDs exhibited either antithixotropic (at low shear rates) or thixotropic (at high shear rates) behavior at different temperatures. Antithixotropic behavior was found in the shear stress range less than 120–150 Pa in all cases. Beyond this shear stress range, the sample showed thixotropic behavior. When sheared in the same range of shear rates (0.1–500 s^{-1}), the sample exhibited greater antithixotropic at higher temperatures, i.e. the anticlockwise loop became bigger in relation to the clockwise loop. The possible reasons for this behavior are: (1) an increase in temperature resulted in a decrease in

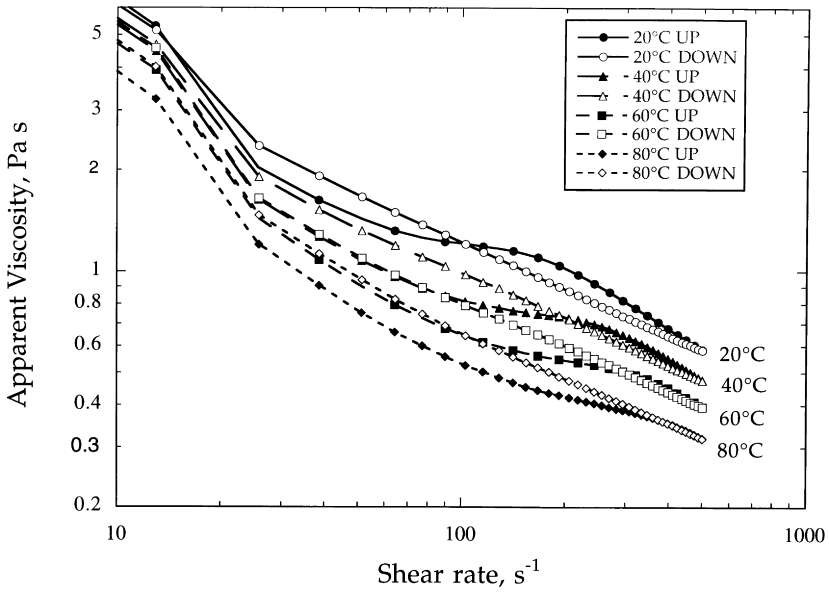

Fig. 4. Shear-thinning (pseudoplastic) and time-dependent shear-thickening behavior of gelatinized 5% cross-linked waxy maize starch dispersions.

shear stress imposed on the sample and, hence, favored antithixotropic; and (2) an increase in temperature resulted in more granule rupture and leaching of amylopectin which facilitated shear-induced structure formation. Antithixotropic behavior of starch dispersions was reported to be related to the shear rate level. Dintzis and Bagley (1995) observed an anticlockwise loop at $\dot{\gamma} < 200\ s^{-1}$ and a clockwise loop at $\dot{\gamma} > 250\ s^{-1}$ in autoclaved 2.0% native waxy maize starch in 0.2 N KOH. 5% gelatinized modified waxy maize starch dispersion exhibited an increase in the antithixotropic behavior when increasing the shear rate from 100 to $200\ s^{-1}$ (Rao et al., 1997). Carriere (1998) reported a critical shear rate for structure formation at $\dot{\gamma} = 50\ s^{-1}$, beyond which shear-thickening behavior was observed in 2% gelatinized waxy maize starch in 90% DMSO, and which decreased when the starch concentration was increased. However, the shear stress values associated with antithixotropic behavior in the above studies agree well with those reported earlier by Härröd and those found in this research (Table 1).

Fig. 6(a) and (b) shows the effect of the maximum shear rate level during a shear cycle on flow behavior of gelatinized CWM STDs. The 5% gelatinized CWM STD showed only antithixotropic behavior, marked by a small anticlockwise loop, when sheared in the range 0.1–40–0.1 s^{-1}. The anticlockwise loop became larger when the sample was

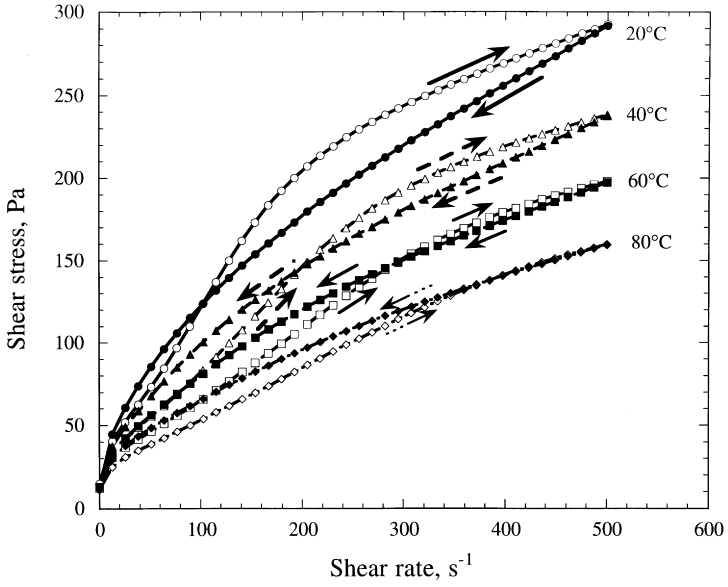

Fig. 5. Thixotropic and antithixotropic behavior of gelatinized 5% cross-linked waxy maize starch dispersions at different temperatures.

Table 1
Shear stress range at which antithixotropic behavior of starch dispersions was observed

Material	Shear stress range (Pa)	Shear rate range (s^{-1})	Reference
1.5–2.5% Gelatinized waxy maize starch in 90% DMSO, 25°C	$0 < \sigma < \sim 100$	$0.1 < \dot{\gamma} < 200\ s^{-1}$ (2&2.5%) and $0.1 < \dot{\gamma} < 500\ s^{-1}$ (1.5%)	Carriere, 1998
Autoclaved 2.6% cross-linked waxy maize starch, 20°C	$0 < \sigma < \sim 150$	$0 < \dot{\gamma} < 1000\ s^{-1}$	Chamberlain, 1996
3% Waxy rice starch in 0.2N NaOH, 25°C	$0 < \sigma < \sim 40$	$0 < \dot{\gamma} < 225\ s^{-1}$	Dintzis et al., 1996
2% (w/v) Waxy maize starch in 0.2N KOH, 30°C	$0 < \sigma < 30$	$0 < \dot{\gamma} < 750\ s^{-1}$	Dintzis and Bagley, 1995
7.7% (w/v) Autoclaved waxy maize starch, 50°C	$0 < \sigma < 150$	$0 < \dot{\gamma} < 750\ s^{-1}$	Dintzis and Bagley, 1995
Maize starch pastes	$30 < \sigma < 100$	Referred in Härröd, 1989.	Doublier, 1987
3%, 5%, 8% Modified potato starch, 10–90°C	$10 \pm 5 < \sigma < 150 \pm 50$	$6 < \dot{\gamma} < 540\ s^{-1}$	Härröd, 1989
5% Modified waxy maize starch, 20°C	~ 90	$\dot{\gamma} = 200\ s^{-1}$ (time sweep test)	Rao et al., 1997
5% Cross-linked waxy maize starch (Purity W®), 20°C	$0 < \sigma < \sim 150$	$0.1 < \dot{\gamma} < 125.7\ s^{-1}$	This work
6% Purity W®, 20°C	$0 < \sigma < \sim 150$	$0.1 < \dot{\gamma} < 40\ s^{-1}$	This work
5% Purity W®, 20, 40, 60, and 80°C	$0 < \sigma < \sim 150$	$0.1 < \dot{\gamma} < 500\ s^{-1}$	This work

sheared in the range 0.1–125–0.1 s^{-1} confirming that the antithixotropic behavior was a result of the shear-induced structure formation.

A different behavior was observed in the gelatinized 6% CWM STD; the 6% sample sheared in the 0.1–40–0.1 s^{-1} shear cycle showed antithixotropic behavior, while that sheared in the 0.1–125–0.1 s^{-1} shear cycle showed thixotropic behavior. When more granules were added to the system by increasing the starch concentration it is likely that: (1) the starch granules absorbed less water and, thus, retained their rigidity and were less likely to be disrupted; as a result, less amount of amylopectin, which is the major reason for shear-induced structure formation (Dintzis et al., 1996), was leached into the continuous phase; and (2) adding more granules resulted in an increase in shear stresses imposed on the system. When the upper critical shear stress was exceeded, antithixotropic behavior was no longer favored.

To further examine the antithixotropic behavior of the gelatinized 5% CWM STD, the procedure of Chamberlain et al. (1999), i.e. shearing the sample for three consecutive shear cycles, was performed. Fig. 7 shows that a higher shear stress versus shear rate curve was obtained during the decreasing-shear portion of each cycle. This indicated that the apparent viscosity of the sample increased with each shearing cycle. Similar behavior was observed in gelatinized 6% CWM STD sheared at the 0.1–40–0.1 s^{-1} shear cycle for three consecutive times (figure not shown). The shear-induced cluster formation which resulted in an

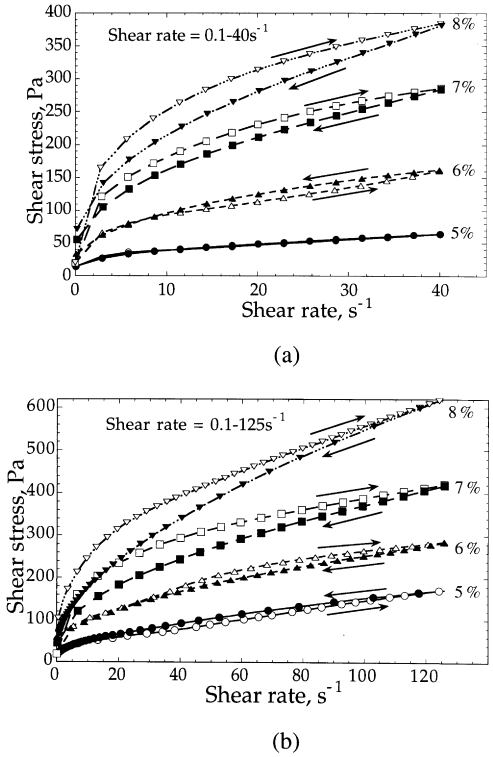

Fig. 6. Effect of shear rate on gelatinized cross-linked waxy maize starch dispersions at different concentrations: (a) shear rate range 0.1–40 s^{-1}; and (b) shear rate range 0.1–125 s^{-1}.

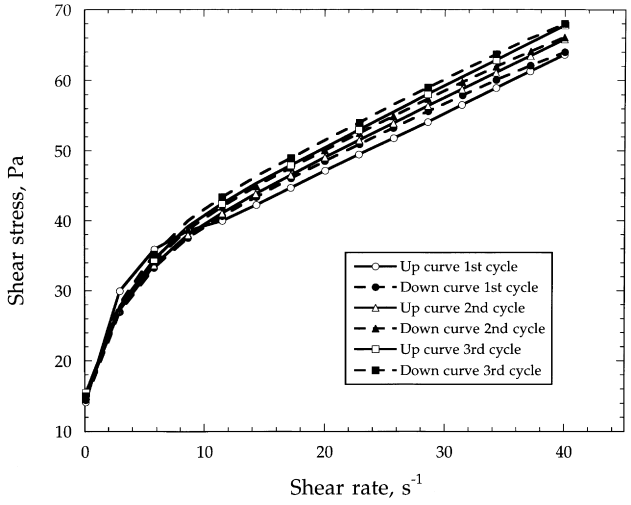

Fig. 7. Effect of shear history on flow behavior of gelatinized 5% cross-linked waxy maize starch dispersion tested at 20°C.

increased apparent viscosity appears to be the reason for such a behavior.

5. Conclusions

Temperature sweep test of cross-linked waxy maize (CWM) starch dispersions showed that 5% (w/w) CMW starch dispersions had a gelatinization onset temperature at 60°C and a peak complex viscosity (η^*_{peak}) of 6.9 Pa s at 64°C. The post-gelatinization viscosity of 5% (w/w) CWM starch dispersions remained relatively high ($\sim 0.85\eta^*_{peak}$ at $\sim$80°C) and remained stable with increasing heating time. A model representing the η^*-T profile of the 5% (w/w) CWM starch dispersions over a wide range of oscillatory shear rates and a temperature range of 55–95°C was obtained. The modified Cox–Merz rule was used to establish the relationship between η^* and η_a. From the two correlations (η^*-T and $\eta^*-\eta_a$), a functional gelatinization model for 5% CWM starch dispersion can be derived. Similar functional models have been used in thermal processing studies on starch dispersions (Liao, 1998; Yang & Rao, 1998b). Flow tests on gelatinized 5% CWM STDs showed that the sample had both time-dependent shear thickening (antithixotropic) and time-dependent shear-thinning (thixotropic) behavior during a full shear cycle. The antithixotropic behavior, which resulted from a shear-induced structure formation, predominated when the level of shear stress imposed on the sample was less than 120–150 Pa.

Acknowledgements

We thank the Royal Thai Government for a scholarship to JT, USDA NRI for grant 97-35503-4493, and the National Starch and Chemical Co. for donation of starch.

References

Barnes, H. A., Hutton, J. F., & Walters, K. (1989). *An introduction to rheology*. Amsterdam: Elsevier.

Carriere, C. J. (1998). Network development during shear-thickening in semidilute solutions of gently solubilized starches. *Journal of Polymer Physics*, *36*, 2085–2093.

Chamberlain, E. K. (1996). *Characterization of heated and thermally processed cross-linked waxy maize starch utilizing particle size analysis, microscopy and rheology*. MS thesis, Cornell University, Ithaca, New York.

Chamberlain, E. K., Rao, M. A., & Cohen, C. (1999). Shear thinning and antithixotropic behavior of a heated cross-linked waxy maize starch dispersion. *International Journal of Food Properties*, *2* (1), 63–77.

Dintzis, F. R., & Bagley, E. B. (1995). Shear-thickening and transient flow effects in starch solutions. *Journal of Applied Polymer Science*, *56*, 637–640.

Dintzis, F. R., Berhow, M. A., Bagley, E. B., Wu, Y. V., & Felker, F. C. (1996). Shear-thickening behavior and shear-induced structure in gently solubilized starches. *Cereal Chemistry*, *73* (5), 638–643.

Dolan, K. D., & Steffe, J. F. (1990). Modeling rheological behavior of gelatinizing starch solutions using mixer viscometry data. *Journal of Texture Studies*, *21*, 265–294.

Doublier, J.-L. (1987). A rheological comparison of wheat, maize, faba bean and smooth pea starches. *Journal of Cereal Science*, *5* (3), 247–262.

Ferry, J. D. (1980). *Viscoelastic properties of polymers*, (3rd ed.). New York: Wiley.

Harper, J. C., & El Sahrigi, A. F. (1965). Viscometric behavior of tomato concentrates. *Journal of Food Science*, *30*, 470–476.

Härröd, M. (1989). Time-dependent flow behavior of starch pastes, with food process applications. *Journal of Food Process Engineering*, *11*, 297–309.

Holmes, Z. A., & Soeldner, A. (1981). Macrostructure of selected raw starches and selected heated starch dispersions. *Journal of American Diet Association*, *78* (2), 153–157.

Kubota, K., Hosokawa, Y., Suzuki, K., & Hosaka, H. (1979). Studies on the gelatinization rate of rice and potato starches. *Journal of Food Science*, *44*, 1394–1397.

Langan, R. E. (1986). Food industry. In O. B. Wurzburg, *Modified starches: properties and uses* (pp. 199–212). Boca Raton, FL: CRC Press.

Liao, H.-J. (1998). *Simulation of continuous sterilization of fluid food products: the role of thermorheological behavior of starch dispersion and process optimization*. PhD thesis, Cornell University, Ithaca, NY.

Lineback, D. R. (1984). The starch granule: organization and properties. *Bakers Digest*, *58* (2), 18–21.

Lineback, D. R. (1986). Current concepts of starch structure and its impact on properties. *Journal of the Japanese Society of Starch Science*, *33* (1), 80–88.

Lund, D. B., & Wirakartakusumah, M. (1984). A model for starch gelatinization phenomena. In M. Mckenna, *Engineering and food: engineering science in the food industry* (pp. 425–432). Vol. 1. New York: Elsevier.

Morgan, R. G., Steffe, J. F., & Ofoli, R. Y. (1989). A gelatinized viscosity model for extrusion of protein doughs. *Journal of Food Process Engineering*, *11*, 55–78.

Okechukwu, P. E., & Rao, M. A. (1995). Influence of granule size on viscosity of corn starch suspension. *Journal of Texture Studies*, *26*, 501–516.

Okechukwu, P. E., Rao, M. A., Ngoddy, P. O., & Mcwatters, K. H. (1991). Flow behavior and gelatinization of cowpea flour and starch dispersions. *Journal of Food Science*, *56*, 1311–1315.

Rao, M. A., Okechukwu, P. E., Da Silva, P. M. S., & Oliveira, J. C. (1997). Rheological behavior of heated starch dispersions in excess water: role of starch granule. *Carbohydrate Polymers*, *33*, 273–283.

Ross-Murphy, S. B. (1984). Rheological methods. In H. W. S. Chan, *Biophysical methods in food research* (pp. 138–199). London: Blackwell Scientific.

Schoch, T. J., & Maywald, E. C. (1968). Preparation and properties of various legume starches. *Cereal Chemistry*, *45*, 564–573.

Swinkels, J. J. M. (1985). Composition and properties of commercial native starches. *Starch/Stärke*, *37* (1), 1–5.

Tattiyakul, J. (2000). *Thermorheology and heat transfer to a canned starch dispersion under agitation: numerical simulation and experiment*. PhD thesis, Cornell University, Ithaca, New York (in preparation).

Vitali, A. A., & Rao, M. A. (1984). Flow properties of low-pulp concentrated orange juice: effect of temperature and concentration. *Journal of Food Science*, *49* (3), 882–888.

Walters, K. (1975). The measurement of the complex dynamic viscosity and related function. In K. Walters, *Rheometry*. London: Chapman and Hall.

Winkler, Von S., Luckow, G., & Donie, H. (1971). Absolute and relative gelatinization characteristics of starch. Part I. Absolute viscosity measuring (Seale Principle). *Starch/Stäerke*, *23*, 325–334.

Yang, W. H., & Rao, M. A. (1998a). Complex viscosity–temperature master curve of cornstarch dispersion during gelatinization. *Journal of Food Process Engineering*, *21*, 191–207.

Yang, W. H., & Rao, M. A. (1998b). Numerical study of parameters affecting broken heating curve. *Journal of Food Engineering*, *37*, 43–61.